VIBRATION CHARACTERISTICS OF QUARTER CAR SEMI-ACTIVE SUSPENSION MODEL - NUMERICAL SIMULATIONS AND INDOOR TESTING

Assist. Prof. Eng. Pavlov N. PhD., Eng. Sokolov E. PhD
Faculty of Transport, Technical University of Sofia, Bulgaria

npavlov@tu-sofia.bg

Abstract: *This paper describes the results of numerical simulations and laboratory experiments of quarter car semi-active suspension model. Elastic characteristic of the coil spring and damping characteristics of the shock absorber in various operating modes are determinate. The amplitude-frequency characteristics and transfer function of the system with various damping coefficient are obtained. The results can be used to design semi-active suspension control strategy for improving ride comfort and road holding of ground vehicles.*

Keywords: VEHICLE, SEMI-ACTIVE SUSPENSION, DAMPING, QUARTER CAR MODEL, RIDE COMFORT

1. Introduction

Automotive suspension there is many conflicting requirements. The suspension characteristics must provide good comfort to passengers when driving on uneven road and at the same time good stability when cornering and braking. Furthermore, it is necessary to ensure optimum contact between the wheels and the road under different driving conditions to achieve maximum safety. Passive suspension used in most modern cars don't provide great opportunities for these conflicting requirements and applying controlled suspension with variable characteristics increase.

By using mechatronic systems with active hydraulic or electric actuators and feedback control is possible to realizate an active suspension which ensures optimum performance in all ride modes [5]. But such type of suspension is more complicated and more expensive than passive, has a high energy consumption and low reliability. Compromise between passive and active is a semi-active suspension, also known as suspension with active damping. This type of suspension consists of a hydraulic controlled damper with variable coefficient of damping and passive elastic element - usually a metal spring. It has reliability close to that of the passive, but offers adaptability of active suspension, with much lower power consumption [3, 10]. Damping characteristics are changed by changing the passage section of the throttling orifice or by changing the viscosity of the hydraulic fluid.

In order to create an algorithm for optimal control of semi-active suspension for various modes of ride and different input disturbance first necessary should to determine the characteristics of its components - springs and adjustable dampers, and vibration characteristics of sprung and unsprung masses.

In this regard, the objective of this publication is the first with the help of laboratory experiments to determine the characteristics of the elements of the suspension and the second using numerical simulations, computer modeling and laboratory experiments on real physical model of the quarter car to determine its vibration characteristics.

2. Spring and damping characteristics

2.1. Spring characteristic

The spring stiffness characteristic has been received on the electro-hydraulic test bench shown in Fig. 1. The test bench is equipped with a force sensor and displacement sensor.

Analysis of the characteristic (Fig. 2) shows that in the separate points, the coefficient of elasticity is obtained between 19,5 and 20,5 kN / m i.e. it can be considered linear. The average value of the spring ratio on five points:

$$c = \frac{F_s}{z} = 20\ kN/m$$

Fig. 1. *Spring characteristic test bench.*

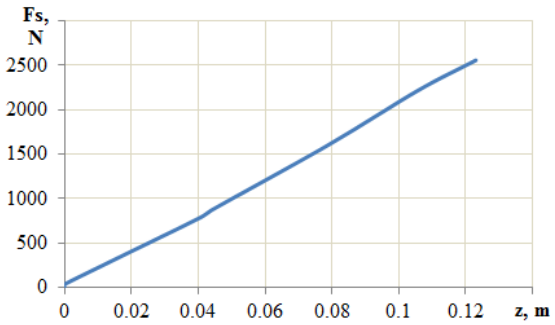

Fig. 2. *Spring stiffness characteristic.*

2.2. Shock absorber characteristics

To obtain force-displacement and force-velocity characteristics of the shock absorber, was used electro-mechanical shock tester, make from Intercomp®, model Shock Dyno - Hi Speed (Fig. 3).

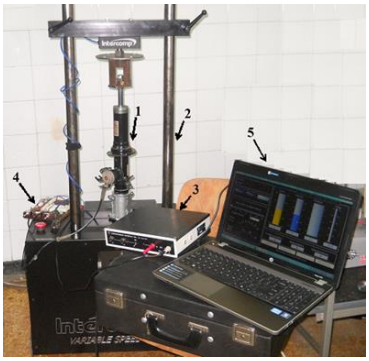

Fig. 3. *Shock absorbers tester.*
1. Adjustable shock absorber; 2. Shock tester; 3. Stabilized DC power supply, U = 12 V; 4. Board with a set of switchable resistors; 5. Laptop.

The stand is factory equipped with displacement sensor, force sensor as well as analog-digital device for collecting data type USB-6009 DAQ from National Instruments®. Visualization and recording the shock absorber characteristics was done using a laptop with special software. The methodology for the obtaining of the characteristics is described in detail in work [8].

Fig. 4 shows the characteristics of the shock absorber tests at different values of current flowing through the solenoid coil (Is). Selected stroke is ± 2,5 cm, and the speed is varied by the step 10 cm/s in the range from 0 to 100 cm/s

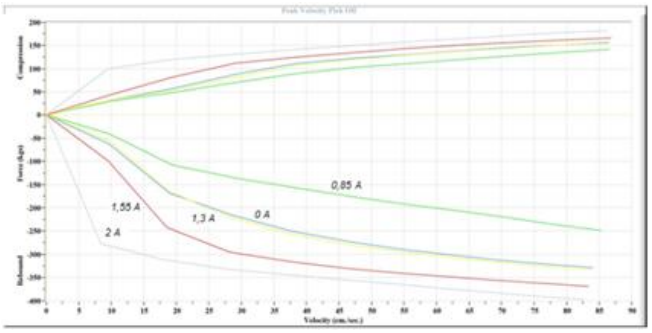

Fig.4. *Characteristics of the adjustable shock absorber with different values of Is.*

In the special literature [7, 3, 11] recommended in initial design calculations of automotive suspension to use damping coefficient at piston speed v = 0,52 m/s. Fig. 5 shows displacement-force diagram for tested shock absorber on piston speed of 52 cm/s and move ± 2,5 cm.

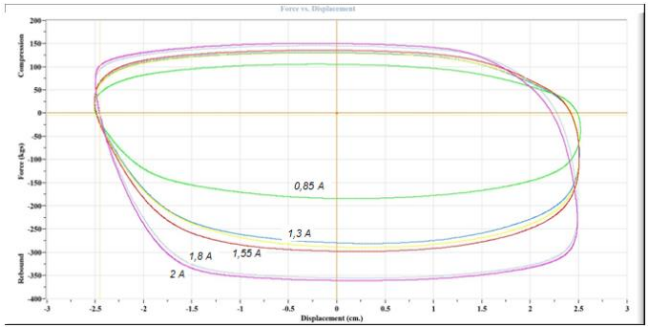

Fig. 5. *Displacement-force characteristic of adjustable shock absorber in piston velocity v = 52 cm / s and different values of Is.*

The calculation damping coefficient of the shock absorber β, is obtained as the arithmetic average of the resistive force of the shock absorber F_{av}, divided by the velocity of the piston, which in this case is 0,52 m/s:

$$\beta = \frac{F_{av}}{v}$$

$$F_{av} = \frac{F_c + F_r}{2}$$

Where F_c and F_r are respectively the resistance forces of the shock absorber during compression and rebound, N.

Asymmetry ratio is:

$$k_a = \frac{F_r}{F_c}$$

Designated parameters of the shock absorber, when the piston speed $v = 0{,}52\ m/s$ and different amperage are shown in Table 1.

Table 1: *Shock absorber parameters in piston velocity mode v=0,52 m/s and different values of current Ic.*

I_s. A	F_{av}, N	β, (N.s)/m	k_a, -
0,85	1425	2740	1,7
1,30	2025	3895	2,2
1,55	2150	4135	2,3
1,80	2475	4760	2,4
2,00	2575	4950	2,4

3. Mechano-mathematical quarter car model

Ride comfort of the car and its operational safety is largely determined by the characteristics of the suspension [9]. Key indicator determining the comfort of motion is the RMS value of the vertical acceleration of the sprung masses $\sigma_{\ddot{z}}$. As additional indicators are used magnitude of maximum vertical acceleration $\pm \ddot{z}_{max}$ [2].

RMS value of acceleration of unsprung masses is an important indicator of road holding as giving us information about dynamic wheel load [9].

To identify these indicators and set at the stage of designing the car it needs to be represented by its mechano-mathematical model. For the modeling of the vehicle vertical oscillations, the most commonly used models shown in Fig. 1. The simplest model is the one with 1 degree of freedom (фиг. 1, a). It takes account unsprung mass ***m*** acting on a one wheel (1/4 of the car mass).

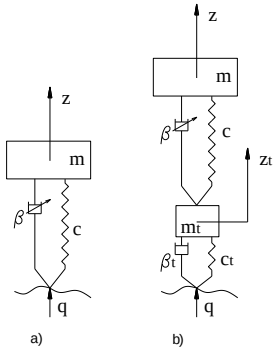

Fig. 6. *1DOF (a) and 2DOF (b) quarter car model.*

More complex is dual mass plane model with two degrees of freedom (фиг. 1, b). It consists of two bodies – sprung mass ***m*** and unsprung mass $\boldsymbol{m_t}$ and two elastic elements ***c*** and $\boldsymbol{c_t}$, representing respectively the elasticity of the main elastic element and the tire elasticity. Dissipative elements are $\boldsymbol{\beta}$ and $\boldsymbol{\beta_t}$ and represent the main dissipative elements (dampers) and tire dissipation. Through this model we receive results for the characteristics of the sprung and unsprung masses.

The basis of the method is Lagrange equation of the second order:

$$\frac{d}{dt}\left(\frac{\partial \mathrm{T}}{\partial \dot{q}_i}\right) - \left(\frac{\partial \mathrm{T}}{\partial q_i}\right) + \left(\frac{\partial \Pi}{\partial q_i}\right) + \left(\frac{\partial R}{\partial \dot{q}_i}\right) = Q$$

wherein T and Π are the kinetic and potential energy of the system;

R – Rayleigh dissipation function;

q_i, $\dot{q}_i$ - vector of generalized coordinates and velocities;

Q – kinematic disturbance;

t – time.

For the model of Fig. 1, a) generalized coordinate and it derivatives are:

$$q = z\ ,\ \dot{q} = \dot{z}\ ,\ \ddot{q} = \ddot{z}\ .$$

Differential equation describing the vibration of the system is:

$$m\ddot{z} + \beta\dot{z} + cz = \beta\dot{q} + cq$$

Apply the transformation of Laplace with zero initial conditions and receive operator images of equation:

$$(mp^2 + \beta p + c)Z(p) - (\beta p + c)Z_t(p) = (\beta p + c)Q(p)$$

where $Z(p)$ and $Q(p)$ are the Laplace transforms (images) of the functions $z(t)$ and $q(t)$; p - complex variable.

It is known that the transfer function of a linear system is the ratio of the Laplacian image to the output variable to the Laplacian image for the input variable, with zero initial conditions [1]. Then the transfer function of the displacements of the sprung and unsprung masses of the system of Fig. 1, a) is given:

$$W_z(p) = \frac{Z(p)}{Q(p)} = \frac{\beta p + c}{mp^2 + \beta p + c}$$

The term transfer function is closely related to the term frequency response (amplitude-phase characteristic [1]). Frequency response of a linear dynamic system is called the transfer function for purely imaginary values of the argument p, i.e. in case of $p = i\nu$, where i is the imaginary unit, and ν is the frequency in rad/s. Then the frequency characteristics are:

$$W_z(i\nu) = \frac{Z(i\nu)}{Q(i\nu)} = \frac{\beta(i\nu) + c}{m(i\nu)^2 + \beta(i\nu) + c}$$

Spectral densities of the displacements and accelerations of the sprung masses are:

$$S_z(\nu) = |W_z(i\nu)|^2 S_q(\nu)$$
$$S_{\ddot{z}}(\nu) = \nu^4 |W_z(i\nu)|^2 S_q(\nu)$$

wherein $S_q(\nu)$ is the spectral density of the input disturbance.

For the model of Fig. 1 b) generalized coordinates and their derivatives are:

$$\{q\} = \begin{bmatrix} z \\ z_t \end{bmatrix};\ \{\dot{q}\} = \begin{bmatrix} \dot{z} \\ \dot{z}_t \end{bmatrix};\ \{\ddot{q}\} = \begin{bmatrix} \ddot{z} \\ \ddot{z}_t \end{bmatrix}.$$

Differential equations describing the oscillations of the system are:

$$m\ddot{z} + c(z - z_t) + \beta(\dot{z} - \dot{z}_t) = 0$$
$$m_t\ddot{z}_t - c(z - z_t) + c_t z_t - \beta(\dot{z} - \dot{z}_t) + \beta_t\dot{z}_t = c_t q + \beta_t\dot{q}$$

After detecting parentheses members are grouped as follows:

$$(m\ddot{z} + \beta\dot{z} + cz) - (\beta\dot{z}_t + cz_t) = 0$$
$$-(\beta\dot{z} + cz) + (m_t\ddot{z}_t + (\beta + \beta_t)\dot{z}_t + (c + c_t)z_t) = \beta_t\dot{q} + c_t q$$

Apply the transformation of Laplace with zero initial conditions and operators receive images of equations:

$$\begin{aligned} &(mp^2 + \beta p + c)Z(p) - (\beta p + c)Z_t(p) = 0 \\ &-(\beta p + c)Z(p) + (m_t p^2 + (\beta + \beta_t)p + c + c_t)Z_t(p) = (\beta_t p + c_t)Q(p) \end{aligned} \quad (1)$$

where $Z(p)$, $Z_t(p)$ and $Q(p)$ are the Laplace transforms (images) of $z(t)$, $z_t(t)$ и $q(t)$.

Then the transfer function of the displacements of the sprung and unsprung masses of the system of Fig. 1, b) as follows:

$$W_z(p) = \frac{Z(p)}{Q(p)};\ W_{zt}(p) = \frac{Z_t(p)}{Q(p)}.$$

To solve the system (1) using the formulas of Kramer for solving systems of linear equations can be written:

$$Z(p) = \frac{\Delta_z}{\Delta};\ Z_t(p) = \frac{\Delta_{zt}}{\Delta},$$

where Δ is the main determinant;

Δ_z - determinant obtained from Δ, by replacing the column of the coefficients before $Z(p)$ with the column of free members (right parts of equations);

Δ_{zt} - determinant obtained from Δ, by replacing the column of the coefficients before $Z_t(p)$ with the column of free members.

Determinants are the following:

$$\Delta = \begin{vmatrix} (mp^2 + \beta p + c) & -(\beta p + c) \\ -(\beta p + c) & (m_t p^2 + (\beta + \beta_t)p + c + c_t) \end{vmatrix}$$
$$\Delta_z = \begin{vmatrix} 0 & -(\beta p + c) \\ (\beta_t p + c_t) & (m_t p^2 + (\beta + \beta_t)p + c + c_t) \end{vmatrix}$$
$$\Delta_{zt} = \begin{vmatrix} (mp^2 + \beta p + c) & 0 \\ -(\beta p + c) & (\beta_t p + c_t) \end{vmatrix}$$

For the transfer functions are obtained:

$$W_z(p) = \frac{Z(p)}{Q(p)} = \frac{(\beta p + c)(\beta_t p + c_t)}{(mp^2 + \beta p + c)(m_t p^2 + (\beta + \beta_t)p + c + c_t) - (\beta p + c)^2}$$

$$W_{zt}(p) = \frac{Z_t(p)}{Q(p)} = \frac{(mp^2 + \beta p + c)(\beta_t p + c_t)}{(mp^2 + \beta p + c)(m_t p^2 + (\beta + \beta_t)p + c + c_t) - (\beta p + c)^2}$$

Then the frequency characteristics are:

$$W_z(i\nu) = \frac{Z(i\nu)}{Q(i\nu)};\ W_{zt}(i\nu) = \frac{Z_t(i\nu)}{Q(i\nu)}.$$

Spectral densities of the displacements and accelerations of the sprung masses are:

$$S_z(\nu) = |W_z(i\nu)|^2 S_q(\nu)$$
$$S_{\ddot{z}}(\nu) = \nu^4 |W_z(i\nu)|^2 S_q(\nu)$$

For the unsprung masses:

$$S_{zt}(\nu) = |W_{zt}(i\nu)|^2 S_q(\nu)$$
$$S_{\ddot{z}t}(\nu) = \nu^4 |W_{zt}(i\nu)|^2 S_q(\nu)$$

4. Numerical experiments

4.1. 1DOF model

Numerical experiments were conducted in MATLAB. The spring ratio of the spring is obtained in section 2.1 - c=20 kN/m, damping parameters are given in Table 1, sprung mass **m** varies in the range of 100-400 kg.

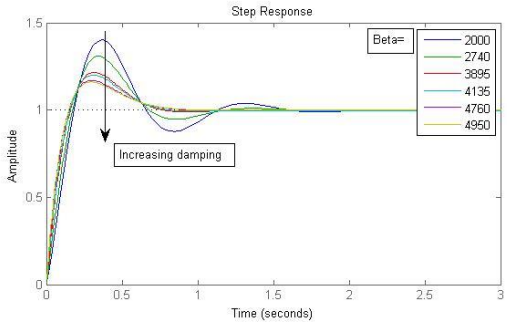

Fig. 7. Oscillogram of 1DOF model damping oscillations at m = 400 kg, and different damping coefficient β.

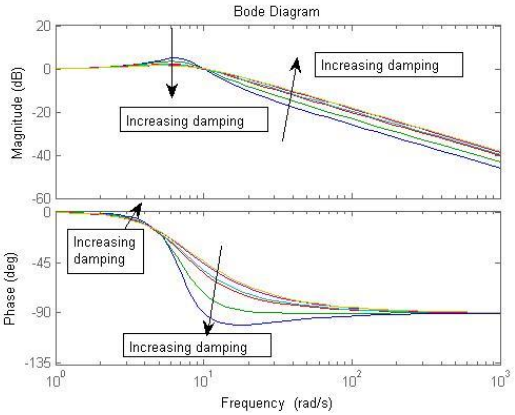

Fig. 8. Amplitude-frequency and a phase-frequency response of 1DOF model at m = 400 kg, and different coefficients β.

4.2. 2DOF model

Unsprung mass is m_t=30 kg, tire spring ratio c_t=150 kN/m, tire damping β_t=50 N.s/m. The other parameters are as 1DOF model.

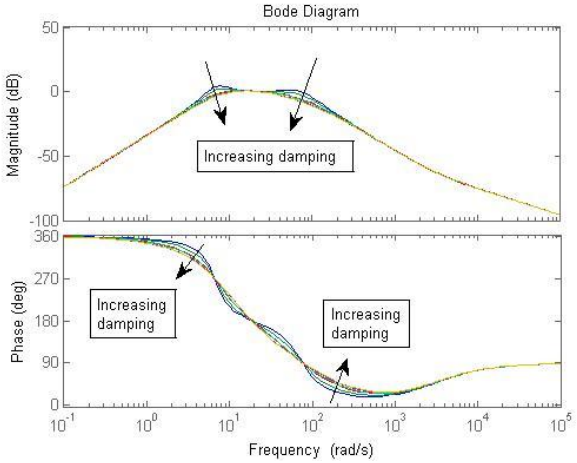

Fig. 9. Amplitude-frequency and a phase-frequency response of 2DOF model at m = 400 kg, and different coefficients β.

Peak of frequency response are at frequencies close to the natural frequency of sprung and unsprung masses.

In a study of random vibrations spectral density of road bumps is set with the [4]:

$$S_q(\nu) = \frac{0{,}000203.0{,}75.1{,}5.\vartheta}{\pi} \cdot \frac{1}{\nu^2 + (1{,}5.\vartheta)^2}$$

where **ν** and **ϑ** are respectively the frequency and velocity of the transport unit.

Spectral density of the calculations in vehicle speed 5 m / s are shown below:

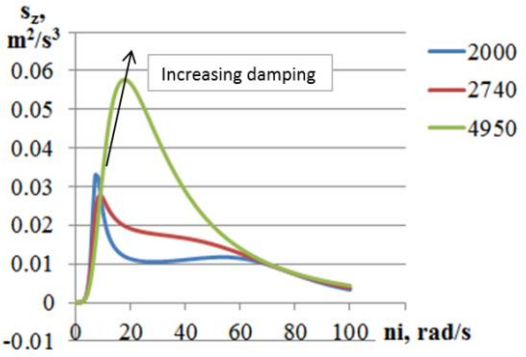

Fig. 10. Spectral density of acceleration of the sprung mass at different values of β.

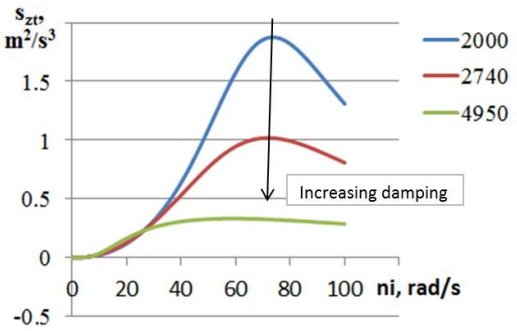

Fig. 11. Spectral density of acceleration of the unsprung masses at different values of β.

Increasing the damping coefficient of the shock absorber adds to the accelerations of the sprung mass resonance in the resonant region, and then slightly reduce the acceleration before reaching the resonant frequency.

By accelerations of unsprung masses noticed a significant reduction in their high rates of resistance to testimony frequency range. The most pronounced is the reduction of the accelerations at the resonant frequency of these tables. Small accelerations testify to small intensity of vibration of the wheels. This is expressed conflicting demands on damping and the need to reduce the coefficient β for maximum comfort and enhancing it in need of maximum contact of the tire and the road.

5. Suspension indoor testing

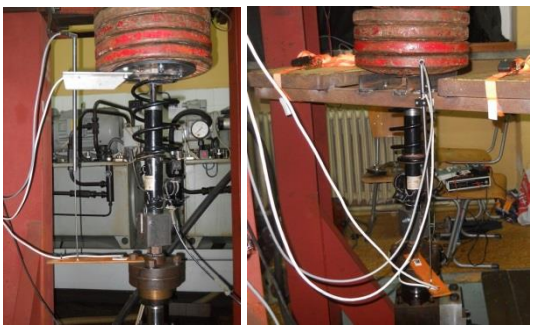

a) *b)*

Fig. 12. Test bench for obtaining vibration characteristics with a load of 100 kg (a) and 160 kg (b).

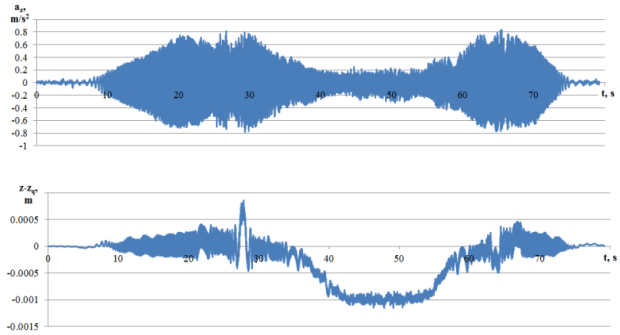

Fig. 13. *Acceleration of the sprung mass and the relative displacement of shifting platform of the test bench with load 100 kg and a growing frequency of 1-20 Hz and decreasing by 20-1Hz.*

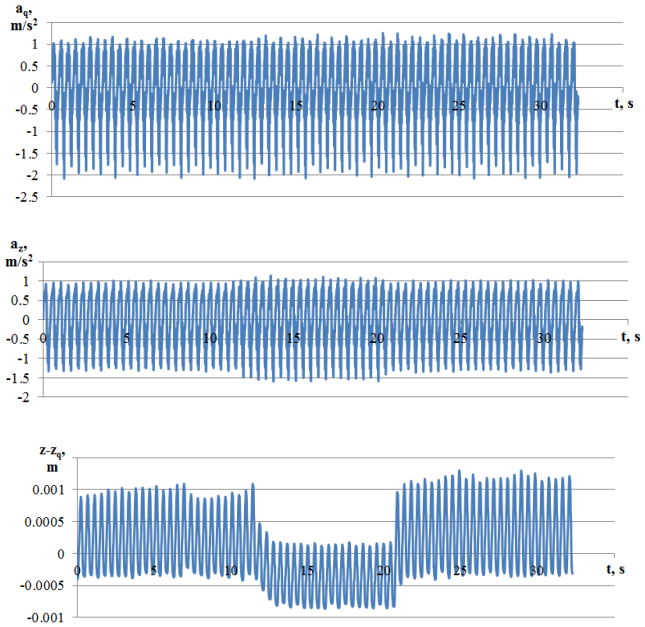

Fig. 14. *Acceleration of the support platform of the test bench, acceleration of the sprung mass and the relative displacement of platform with load of 100 kg and frequency of 3 Hz. The coefficient β changes from 2740 to 4950 (app.10 s) and from 4950 to 2740 N.s / m (app. 20 s).*

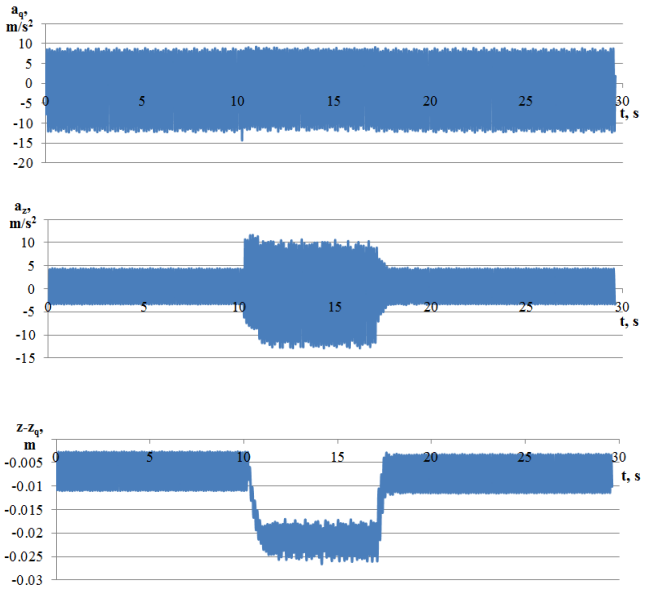

Fig. 15. *Acceleration of the support platform of the test bench, acceleration of the sprung mass and the relative displacement of platform with load of 160 kg and frequency of 8 Hz. The coefficient β changes from 2740 to 4950 (app.10 s) and from 4950 to 2740 N.s / m (app. 20 s).*

Analysis of the results indicates that the system is linear, since the gradual increase in the frequency of interference and consequent reduction, the maximum amplitude of resonant modes is approximately equal (Fig. 13). On the same figure is significantly shifting the zero line of oscillations in after resonance mode. It is due to the gravity of the sprung mass down, due to the asymmetric damping. As a result, the dynamic vertical coordinate of the sprung masses (car body) is reduced and increases the likelihood of impact of the suspension travel of the vehicle and of appearance etc. "Breakthrough" in the suspension, which is felt by the driver and passengers in the car as hard blow when passing through bumps.

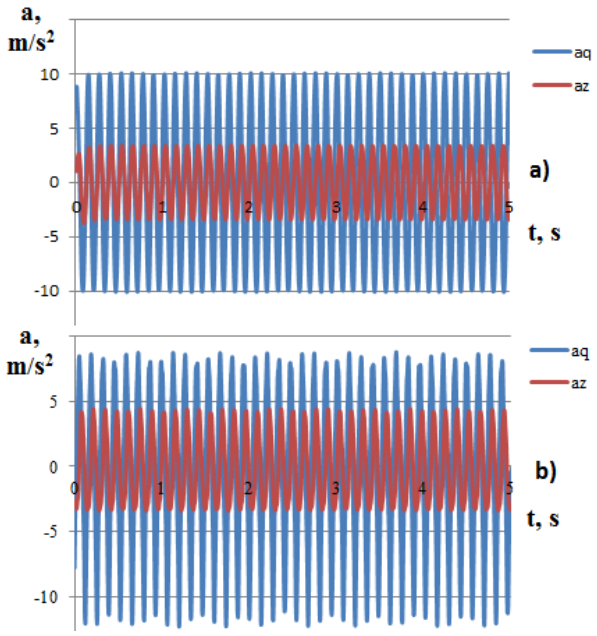

Fig. 16. *Acceleration of the vibration platform (a_q) and sprung mass (a_z), at frequency 8 Hz, m=160 kg and amplitude q_0=4 mm, numerical modeling (a) and laboratory experiment (b).*

Analysis of the results indicates that the system is linear, since the gradual increase in the frequency of interference and consequent reduction, the maximum amplitude of resonant modes is approximately equal (Fig. 13). On the same figure is significantly shifting the zero line of oscillations in after resonance mode. It is due to the gravity of the sprung mass down, due to the asymmetric damping. As a result, the dynamic vertical coordinate of the sprung masses (car body) is reduced and increases the likelihood of impact of the suspension travel of the vehicle and of appearance etc. "Breakthrough" in the suspension, which is felt by the driver and passengers in the car as hard blow when passing through bumps.

Fig. 14 and Fig. 15 shows changes that occur in the same size and frequency of impacts and changing the resistance coefficient of the shock absorber. Sizes acceleration of unsprung mass change, it is more significant at high frequencies and observe the "pull" of unsprung mass down at a high coefficient of resistance again more pronounced at high frequencies of impacts. At 8 Hz (Fig. 15) its value is about 1,5 cm.

Fig. 16 there is a better comparability of results of numerical and laboratory experiments using deterministic sinusoidal disturbance.

5. Conclusion

The considered models and presented laboratory equipment, enable determination of a series of vibration characteristics of semi-active suspension. Results of waveforms for free damped oscillations amplitude- and phase-frequency characteristics, spectral density of acceleration and other characteristics of the forced vibrations with deterministic or random nature. The results of numerical modeling have good compatibility with those of laboratory experiments and can be used to compile algorithms and

control strategies of semi-active suspension to improve the comfort and road holding of the road vehicles.

Acknowledgement

The research presented in this article received financial support from the Scientific and Research Sector of the Technical University of Sofia – Internal Funding Session 2016. Contract № 161ПР0002-04.

Reference:

[1]. Ищев. К. Г. Теория на автоматичното управление. ТУ-София, 2007.

[2]. Кунчев, Л. П. Динамика на автомобилната техника. Ръководство за лабораторни упражнения. ТУ-София, 1997.

[3]. СТ на СИВ 3044-81. Амортисьори телескопични хидравлични автомобилни. Методи за стендови изпитвания. София, и-во Стандартизация, 1983.

[4]. Успенский, И. Н. Проектирование подвески автомобиля. М., Машиностроение, 1976.

[5]. Fijalkowski B. T. Automotive Mechatronics: Operational and Practical Issues: Volume II. Springer, 2011.

[6]. Guglielmino, E., T. Sireteanu. Semi-active Suspension Control: Improved Vehicle Ride and Road Friendliness. Springer, 2008.

[7]. Heißing, B. Chassis Handbook: Fundamentals, Driving Dynamics, Components, Mechatronics, Perspectives. Wiesbaden, Vieweg+Teubner Verlag, 2011.

[8]. Pavlov, N. A Method and Test Equipment for Obtaining Characteristics of Controlled Hydraulic Shock Absorbers. EKO Varna, 2015.

[9]. Robert Bosch GmbH, Automotive Handbook, 2002.

[10]. Sireteanu, T. Damping Optimization of Passive and Semi-active Vehicle Suspension by Numerical Simulation. Proceedings of the Romanian Academy, 2003.

[11]. ZF Sachs: Technisches Handbuch für den Konstrukteur (Kraftfahrzeugstoßdämpfer).